

# HfC-based coating prepared by reactive melt infiltration on C/C composite substrate

Yicong Ye\*, Hong Zhang, Yonggang Tong, Shuxin Bai

*College of Aerospace Science and Engineering, National University of Defense Technology, Changsha 410073, PR China*

Received 15 November 2012; received in revised form 14 December 2012; accepted 14 December 2012

Available online 28 December 2012

## Abstract

Reactive melt infiltration based on alloy design is proposed in the present work for preparing HfC-based coating on C/C composite substrate. A 50Hf10Zr40Si alloy ingot was prepared and infiltrated into a C/C preform at temperatures much lower than the melting point of the alloy to obtain the HfC-based coating. An obvious layered microstructure of the coating was formed. The carbonization reactions occurring between Hf and carbon of the surface layer of the C/C composite is the primary reason for the reactive melt infiltration process to proceed at relative low temperatures. Acetylene flame test showed that the HfC-based coating protected the C/C composite from serious oxidation.

© 2012 Elsevier Ltd and Techna Group S.r.l. All rights reserved.

*Keywords:* HfC; Coating; Reactive melt infiltration; C/C composite

## 1. Introduction

Ultrahigh temperature materials (UHTMs) capable of prolonged operation in oxidizing environments at temperatures above 2000 °C are required for future space systems [1]. Carbon/carbon (C/C) composite is one of the most widely studied and developed UHTMs due to its excellent properties such as low density, high specific strength, high thermal conductivity, and high resistance to thermal shock [2]. Nevertheless, C/C composites begin to oxidize over 400 °C in oxidizing environments and cannot meet the requirements any more at ultrahigh temperatures [3]. To improve the oxidation resistance of C/C composites, preparing protective coating on the surface of C/C composites is the most promising method [4,5]. Carbide coatings for protecting C/C composite from oxidation and ablation have been widely studied [6–8]. Hafnium (Hf) is a strong carbide forming element. Due to the very high melting points of HfC and HfO<sub>2</sub> and the relative low evaporation rate of HfO<sub>2</sub> [9], the HfC-based

coating is a very promising candidate for protecting C/C composites from oxidation and ablation.

Reactive melt infiltration (RMI) is an effective method to introduce refractory carbide compounds into C/C preform. Infiltrated metal melt reacts with the already existing carbon in the C/C preform to form the ceramic matrix. The driving force for infiltration is capillarity. RMI is of short fabrication period and low cost and is generally used to prepare carbon fiber reinforced ceramic matrix composite [10–12]. According to the characteristics of RMI process, it is believed that RMI is also suitable for preparing carbide coating on C/C substrates by controlling the infiltration depth of melts, which has not yet been reported anywhere up to now. In this paper, RMI based on alloy design is used to prepare HfC-based coatings of different thicknesses on C/C composite substrates. Due to the high melting point of pure hafnium (2233 °C), RMI for preparing HfC coating should be conducted above 2300 °C, which is not easy and will do harm to the mechanical properties of carbon fibers. Alloy design can be applied to decrease the processing temperature of RMI and to introduce more effective components for anti-oxidation. By RMI based on alloy design, the HfC-based thick coating can be obtained very quickly and at a relative

\*Corresponding author. Tel.: +86 731 84573180; fax: +86 731 84574791.  
E-mail address: [yeyicong@gmail.com](mailto:yeyicong@gmail.com) (Y. Ye).

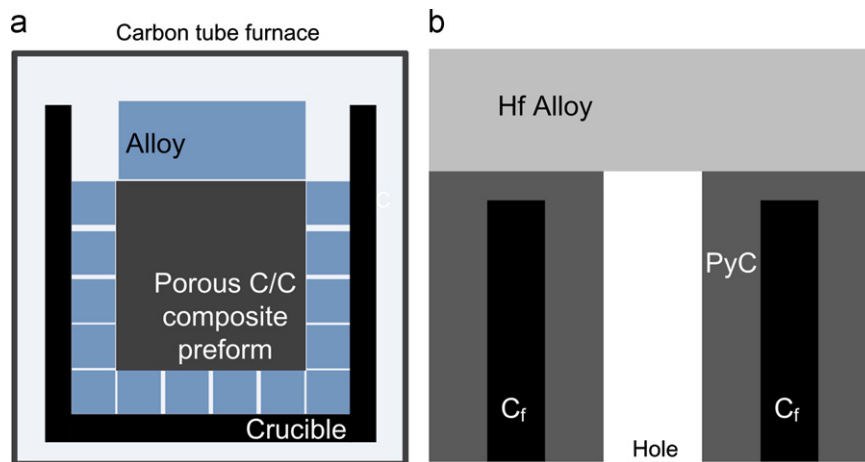


Fig. 1. (a) The alloy ingot were placed surrounding the C/C composite, which was heated up to 1600–1900 °C, holding for 30 min, followed by furnace cooling; (b) details of the RMI process—PyC means pyrolytic carbon and C<sub>f</sub> means carbon fiber.

low temperature, which is also beneficial for cost reduction.

## 2. Experimental

A 50Hf10Zr40Si alloy ingot was designed, prepared and smashed into small pieces. Alloy design will be discussed later in this paper. A porous C/C composite preform and the alloy pieces were put into a graphite crucible, which was then placed in a carbon tube furnace with a vacuum degree of  $10^{-2}$  Pa and heated up to 1600 °C, 1700 °C and 1900 °C, correspondingly, holding for 30 min, followed by furnace cooling (Fig. 1a). After the completion of reactive melt infiltration (RMI) process (Fig. 1b), the sample covered by HfC-based coating were obtained. The sample was examined by X-ray diffraction (XRD), field emission scanning electron microscopy (FESEM), and energy dispersive spectroscopy (EDS) to determine its phase composition, constituent and microstructure. Acetylene flame was applied to test the anti-oxidation performance of the C/C composite with HfC-based coating. The temperature of the sample being tested was around 1800 °C. The test lasted for 10 min.

## 3. Alloy design and preparation

Alloy design is a key step during the RMI process for preparing HfC-based coating. The composition of Hf alloy is designed as follows. Multiphase ultrahigh ceramics possess high resistance to oxidation and ablation. It is reasonable to design the Hf alloy based on the relative mature ultrahigh temperature ceramic system. Multiphase ceramic  $\text{HfB}_2(\text{ZrB}_2)\text{--}20\%\text{SiC--}20\%\text{TaSi}_2$  prepared by hot pressed sintering kept undamaged at 1627 °C for a long duration [13]. The anti-ablation property of the ceramic comes from the anti-oxidation property of oxides of different metals. Oxides of alloy elements play different roles during the ablation process.  $\text{HfO}_2$ , with the melting

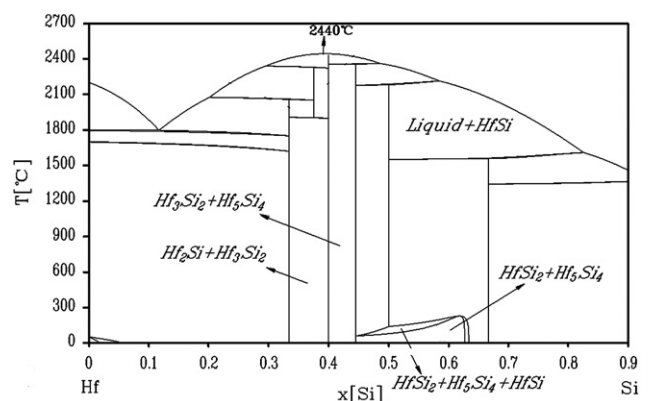


Fig. 2. The 10 at% Zr longitudinal section of the Hf–Zr–Si ternary phase diagram (at% calculated using Pandat<sup>®</sup>).

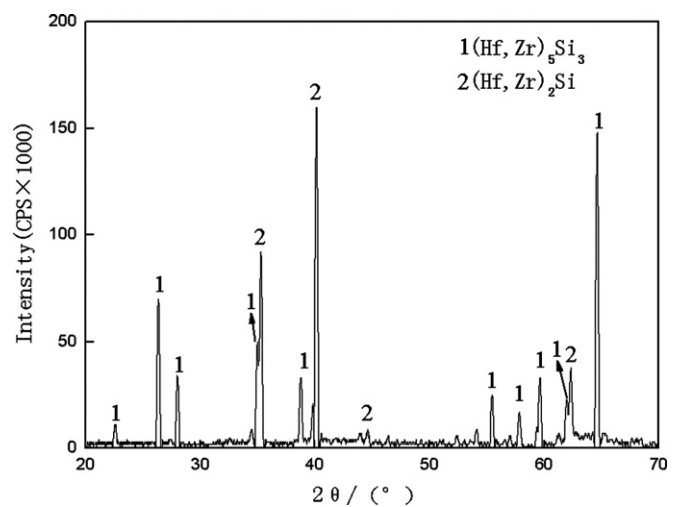


Fig. 3. XRD analysis result of the 50Hf10Zr40Si alloy.

point of 2810 °C, is the main ultrahigh temperature phase and can bear scouring of high temperature gas flow.  $\text{ZrO}_2$ , with the melting point of 2700 °C, is also an important

ultrahigh temperature phase. Solid solution of unlimited mutual solubility between  $ZrO_2$  and  $HfO_2$  can be formed.  $SiO_2$ , with the melting point of  $1728\text{ }^\circ\text{C}$ , converts to melt of certain viscosity at high temperatures. The melt of  $SiO_2$  possesses good infiltrating performance, very low oxygen permeability and can spread out and form an intact silicate film on the surface of the matrix. This film will heal cracks formed due to thermal mismatch and pores generates as gas escapes. It was decided that the elements of the designed alloy included Hf, Zr and Si with a mole ratio of 50:10:40. The Hf content was not less than 50 at% because the HfC-based coating was expected to be applied in higher temperature environment. The silicon content should not be too high, because  $SiO_2$  evaporates seriously at ultrahigh temperature, which should be avoided. Zirconium was added into the alloy to form ZrC during RMI, also decreasing the melting point of the alloy.

The 10 at%Zr longitudinal section of the Hf–Zr–Si ternary phase diagram is shown in Fig. 2, which was calculated using phase diagram calculating software Pandat<sup>®</sup>. At room temperature, the 50Hf10Zr40Si alloy of equilibrium state consists mainly of linear compound  $(Hf,Zr)_3Si_2$  and  $(Hf,Zr)_2Si$  phases. The melting point of the alloy is  $2440\text{ }^\circ\text{C}$ . The XRD analysis result (Fig. 3) shows that the alloy consists of the  $(Hf,Zr)_2Si$  phase and  $(Hf,Zr)_5Si_3$  phase. The high-temperature phase  $(Hf,Zr)_5Si_3$  results from non-equilibrium solidification.

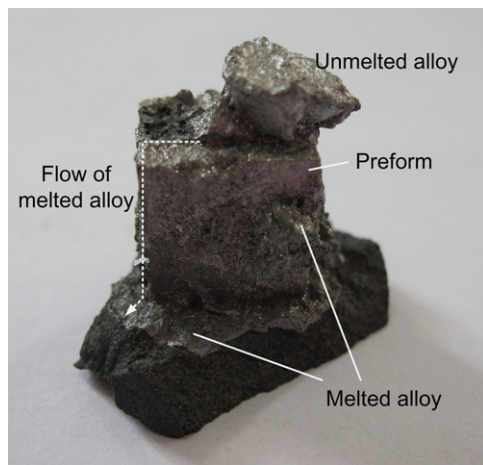


Fig. 4. The appearance of the RMI sample. The melting alloy flew to the side face, covering the whole surface of the composite.

#### 4. Results

It is generally believed that the temperature must be higher than  $2500\text{ }^\circ\text{C}$  for the RMI process to proceed because the melt point of the alloy is  $2440\text{ }^\circ\text{C}$ . However, in the present work, at the process temperature of only  $1600\text{--}1900\text{ }^\circ\text{C}$ , the RMI process definitely occurred, which is discussed as follows.

The sample was taken out of the furnace after heat preservation at  $1900\text{ }^\circ\text{C}$  for 30 min (Fig. 4). Part of the alloy ingot adjacent to the surface of the C/C composite underwent melting. The melted alloy flew to the side face from the top of the sample and covered the whole surface of the composite, leaving a piece of unmelted alloy on top of the composite, which also indicated that the melting point of the alloy was higher than  $1900\text{ }^\circ\text{C}$ . Similar phenomenon was also observed for the  $1600\text{ }^\circ\text{C}$  and  $1700\text{ }^\circ\text{C}$  experiments. The cross sections of the samples were observed under SEM (Fig. 5). A white dense coating was found on the surface of each sample and was variable

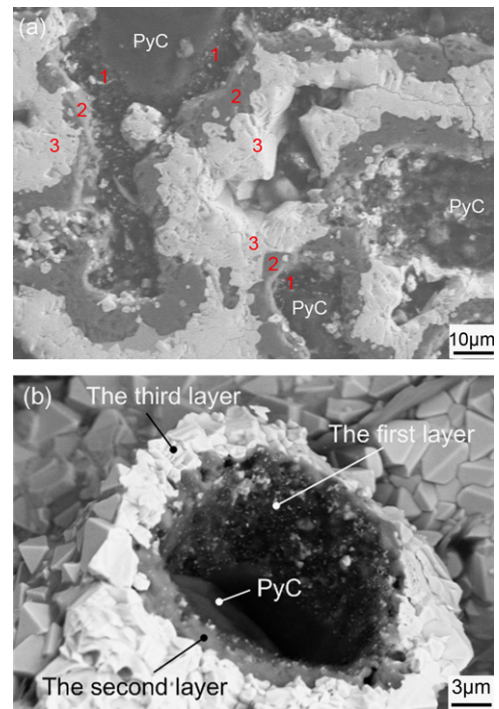


Fig. 6. Microstructures of the RMI sample under SEM: (a) backscattered electron image; and (b) fracture morphology.

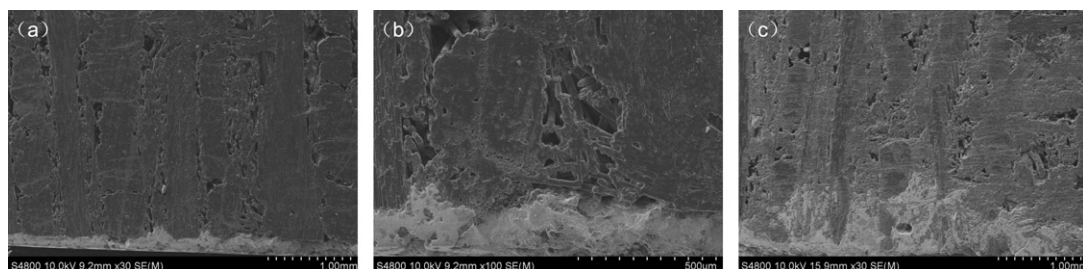


Fig. 5. Cross-section of the samples after RMI process of (a)  $1600\text{ }^\circ\text{C}$ , (b)  $1700\text{ }^\circ\text{C}$  and (c)  $1900\text{ }^\circ\text{C}$ .

in thickness. The average coating thicknesses of the 1600 °C and 1700 °C sample are around 100 μm and 150 μm, respectively, while it is near 500 μm for the 1900 °C sample. The infiltration rates of the melt are different at different temperatures.

An obvious characteristic of the RMI coating structure is shown both in the backscattered electron image (Fig. 6a) and in the fracture micrograph (Fig. 6b), i.e., there are three layers distributing successively in the filled-up holes from the pyrolytic carbon interface toward the central part of the holes. In the first layer (marked by “1” in Fig. 6a), white particles ( $\Phi$ : 1–5 μm) distribute in a dark matrix close to the pyrolytic carbon (PyC) interface. The second layer (marked by “2”) is continuous smooth dark substance. The third layer (marked by “3”) consists of close packing white grains (size: 5–20 μm) with a small quantity of dark inclusions distributing at grain boundary areas. EDS analysis of a typical area (Fig. 7) combined with the known possible reactions of the system indicates that the dispersed white fine particle is HfC or ZrC, the medium size and large size white particles are either HfC or ZrC, the medium size and large size white particles are either HfC or ZrC, and the dark substance is SiC. XRD analysis indicates that the RMI composite is composed of HfC, ZrC and SiC (Fig. 8). No dissociative component was found.

After 10 min ablation, a relative compact film was formed on the surface of the sample (Fig. 9), protecting the sample from further ablation. Micro-morphology of the film is shown in Fig. 10. The film is compact and uniform, few cracks can be seen and micro-crack does not extend because the film tends to convert to glass phase during testing. XRD analysis result (Fig. 10) shows that the phase of the film is mainly monoclinic linear compound (Hf,Zr)O<sub>2</sub>.

## 5. Discussions

### 5.1. Mechanism of preparation of the HfC-based coating

Consider 1900 °C sample as an example. The RMI process occurred at temperatures below the melting point of the alloy. It is supposed that some instantaneous liquid

generated and infiltrated into the composite. This phenomenon could be due to carbonization reactions occurring between the alloy and the carbon in the surface layer of

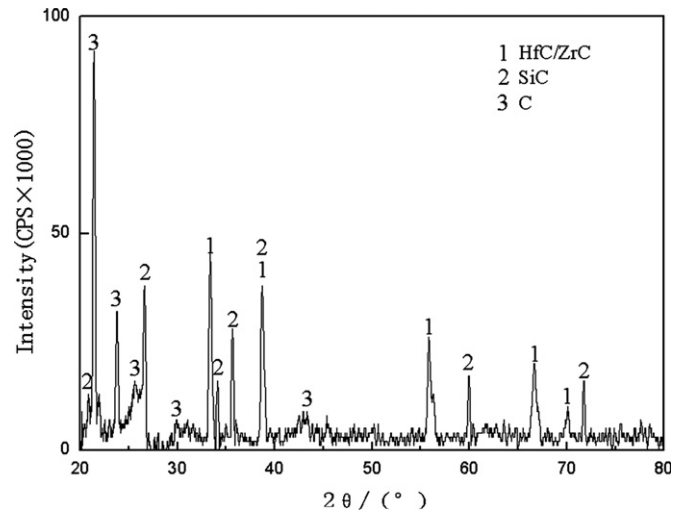


Fig. 8. XRD analysis result of the RMI sample.



Fig. 9. The composite sample after the acetylene flame test for 10 min.

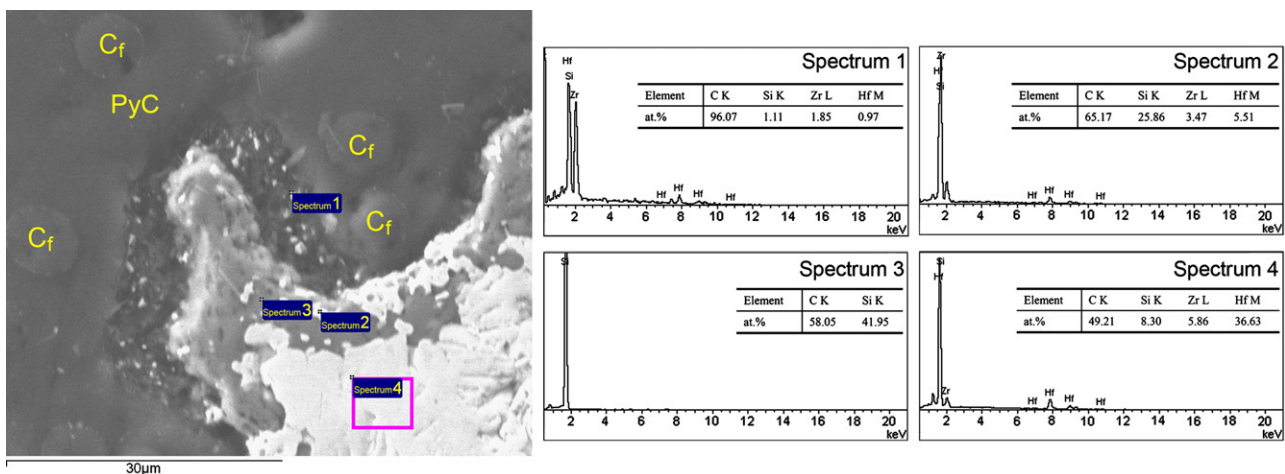


Fig. 7. EDS analysis results of a typical area of the three-layer structure.

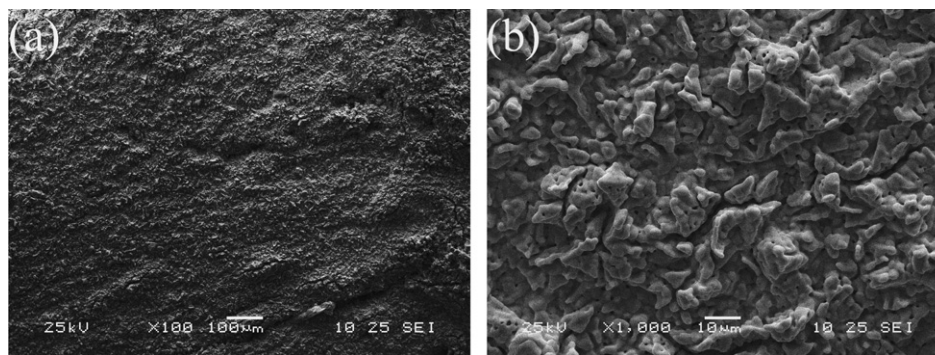


Fig. 10. Micro-morphology of the film on the surface of the sample after ablation: (a) low magnification; and (b) high magnification.

Table 1

The most possible reactions with their Gibbs free energy between  $\text{Hf}_2\text{Si}$  or  $\text{Hf}_5\text{Si}_3$  and carbon at 1900 °C.

No.	Reaction equation	$\Delta G$ (J/mol)
1	$\text{Hf}_2\text{Si}(\text{s}) + 2\text{C}(\text{s}) = 2\text{HfC}(\text{s}) + \text{Si}$	-204,624
2	$\text{Hf}_5\text{Si}_3(\text{s}) + \frac{7}{2}\text{C}(\text{s}) = \frac{3}{2}\text{HfSi}_2(\text{s}) + \frac{7}{2}\text{HfC}(\text{s})$	-585,342
3	$\text{HfSi}(\text{s}) + \text{C}(\text{s}) = \text{HfC}(\text{s}) + \text{Si}$	-55,024

the composite. Because of the very strong carbide-forming ability of Hf, none but the Hf component took part in the carbonization reactions at the beginning, leading to a phase composition change of the alloy at the interface. Instantaneous liquid phase generated from the phase transformation, infiltrated into the C/C composite and reacted with the pyrolytic carbon (PyC), thus the HfC-based coating was obtained. More detailed calculation and analysis are as follows.

The Gibbs free energies of all possible reactions between the initial alloy and carbon were calculated. The initial phases of the alloy are  $(\text{Hf,Zr})_2\text{Si}$  and  $(\text{Hf,Zr})_5\text{Si}_3$ . It is reasonable to simplify the reactants of the carbonization reactions to be just  $\text{Hf}_2\text{Si}$  and  $\text{Hf}_5\text{Si}_3$ . The most possible reactions between these two phases and carbon in the surface layer of the composite (Reaction 1 and 2) at 1900 °C are listed in Table 1. HfC is the product of both Reaction 1 and 2, which generates in the form of small particle. The product of Reaction 1, silicon, is liquid at the processing temperature. The HfC particles will move inside the C/C preform, together with liquid Si infiltrating into the composite. The product of Reaction 2,  $\text{HfSi}_2$ , decomposes to 24 at% Hf (liquid) and HfSi (solid) at temperatures above 1553 °C. If enough carbon is supplied, HfSi will continue to react with carbon in terms of Reaction 3 in Table 1, product of which is HfC and liquid Si. Therefore, due to the carbonization reactions occurring in the surface layer of the composite, liquid phase, including liquid Si and liquid 24 at% Hf–Si, is generated and infiltrates into the composite, where plenty of PyC is supplied. At first, the Hf component reacts with C and HfC is generated, not distinguished with the small HfC particles generated from Reaction 1 and 2. As the Hf component exhausts, SiC

Table 2

Free energies of formation of various carbides at 1900 °C [14].

Carbide	A	B	$\Delta G^\ominus = A + BT$ (KJ mol <sup>-1</sup> )
HfC	-230,100	7.53	-213.74
ZrC	-196,650	9.20	-176.66
SiC	-122,600	37.03	-42.134

Table 3

Possible reactions during the ablation process of the C/C composite coated by HfC-based ceramics.

No.	Reaction equations
1	$\text{HfC}(\text{s}) + \frac{3}{2}\text{O}_2(\text{g}) = \text{HfO}_2(\text{s}) + \text{CO}(\text{g})$
2	$\text{HfO}_2(\text{s}) = \text{HfO}_2(\text{l})$
3	$\text{HfO}_2(\text{l}) = \text{HfO}_2(\text{g})$
4	$\text{ZrC}(\text{s}) + \frac{3}{2}\text{O}_2(\text{g}) = \text{ZrO}_2(\text{s}) + \text{CO}(\text{g})$
5	$\text{ZrO}_2(\text{s}) = \text{ZrO}_2(\text{l})$
6	$\text{ZrO}_2(\text{l}) = \text{ZrO}_2(\text{g})$
7	$\text{C}(\text{s}) + \frac{1}{2}\text{O}_2(\text{g}) = \text{CO}(\text{g})$
8	$\text{CO}(\text{g}) + \frac{1}{2}\text{O}_2(\text{g}) = \text{CO}_2(\text{g})$
9	$\text{SiC}(\text{s}) + \frac{3}{2}\text{O}_2(\text{g}) = \text{SiO}_2(\text{s}) + \text{CO}(\text{g})$
10	$\text{SiO}_2(\text{s}) = \text{SiO}_2(\text{l})$
11	$\text{SiO}_2(\text{l}) = \text{SiO}_2(\text{g})$

starts to form. The HfC and SiC phase forms quickly in the surface layer of the composite, locating on the way of the infiltrating process and expanding, which prevents the melt to continue to infiltrate. Simultaneously, the HfC-based coating with thickness of about 500 μm is obtained. This process is described in Fig. 12. It is suggested that by altering the processing temperature and alloy constituent, coatings of different thickness can be prepared, which will be further investigated in future work.

It is remarkable that the Zr and Si components of the alloy do not take part in the surface carbonization reaction, which is due to the different carbide-forming ability of the components of the alloy. Hf, Zr and Si are all strong carbide forming elements, however, Hf is most easy to form carbide, because the free energy of HfC is the lowest, much lower than that of SiC (Table 2). This is vital for the liquid infiltration process to proceed, because if all

the components react synchronously with carbon in the surface area, only the carbide product and initial alloy will exist on the interface without any liquid phase generating, thus the RMI will not be realized and there is no chance to obtain the thick HfC-based coating.

### 5.2. The anti-ablation mechanism of the coated sample

The sample exhibits excellent oxidation-resistant and ablation-resistant properties because of the behavior of various oxides formed during the ablation. The surface layer of the sample is composed of HfC, SiC, ZrC and C, whose evolution

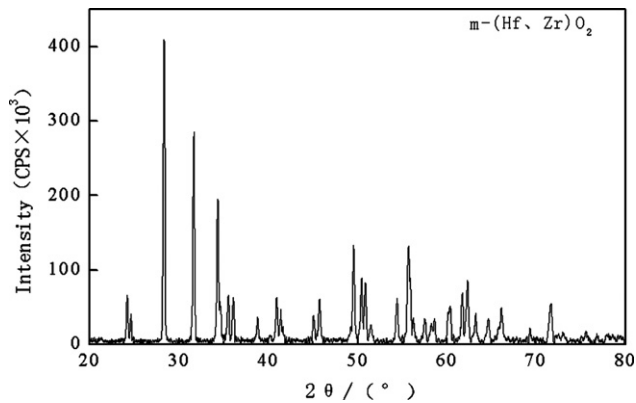


Fig. 11. XRD analysis result of the film on the surface of the sample after ablation.

during ablation is shown as the reaction equations in Table 3.  $\text{SiO}_2$ ,  $\text{HfO}_2$  and  $\text{ZrO}_2$  generate from the oxidation of HfC, ZrC and SiC. No  $\text{SiO}_2$  was found in the surface layer of the tested sample (Fig. 11). At 1800 °C,  $\text{SiO}_2$  evaporated significantly. A large amount of heat was taken away with the melt and evaporation of  $\text{SiO}_2$ . The stable (Hf,Zr) $\text{O}_2$  phase generates as a barrier layer of oxygen on the surface of the sample and protects the sample from further ablation.

Fig. 13 shows the micro-morphology below the surface film of the tested sample (top view). A poriferous skeleton was formed (Fig. 13a). Unconsolidated material of light gray accumulated discontinuously at the upper part of the skeleton (Area A in Fig. 13b), which was composed of Hf, Zr and O. Below it, a dark gray smooth layer formed as the main part of the skeleton (Area B in Fig. 13b), which was mainly composed of Si, Zr and O. It is supposed that the main phases of the skeleton are oxides of Hf and Zr,  $\text{SiO}_2$  and minor  $\text{ZrSiO}_4$ , which needs further observation.

## 6. Conclusions

HfC-based thick coating has been prepared by reactive melt infiltration (RMI) based on alloy design on a C/C composite substrate. The 50Hf10Zr40Si alloy was designed, prepared and used for the RMI. The primary reason for the RMI process to proceed at temperatures much lower than the alloy melting point is that the Hf

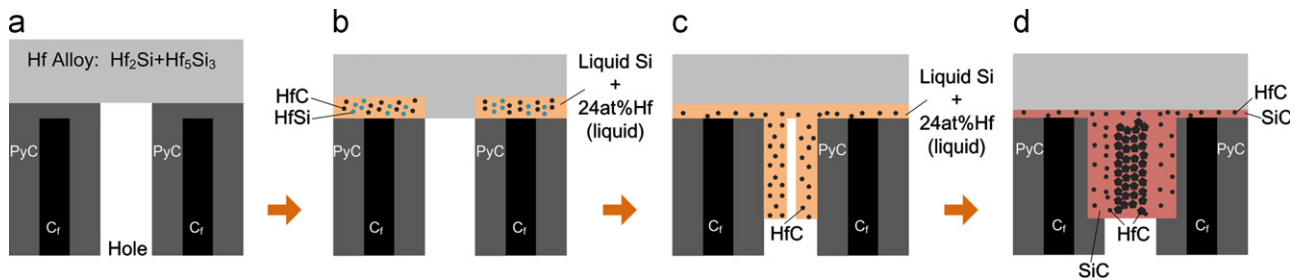


Fig. 12. Sketch of the RMI process: (a) the C/C preform and the alloy for RMI are both heated; (b) the carbonization reactions occur at the surface area of the preform, generating liquid phase and HfC and HfSi particles; (c) the liquid phase infiltrates into the holes in the preform together with the HfC particles, and the HfSi phase transforms to HfC; (d) as the Hf component exhausts and HfC particles coarsen, SiC starts to form as a continuous matrix. The HfC and SiC phases locate on the way of the infiltrating process and expend, preventing the melt to continue to infiltrate.

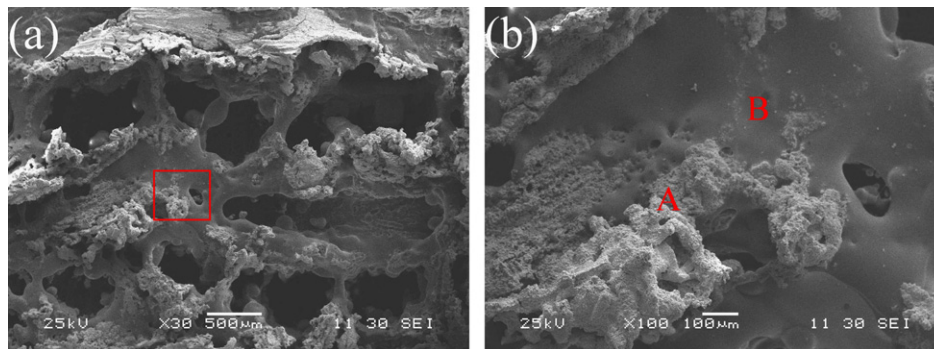


Fig. 13. Micro-morphology below the surface film of the tested sample (top view): (a) a poriferous skeleton was formed; and (b) magnified image of the rectangle area in (a).

component has a very strong carbide-forming ability, and the carbonization reactions occur between Hf and carbon of the surface layer of the C/C composite. Different products formed at different stages of the carbonization reactions and generation of the liquid phases result in the formation of the special layered RMI microstructure. After 10 min ablation, a relative compact film was formed on the surface of the sample, protecting the sample from further serious ablation. The sample exhibits a relative high resistance to oxidation because of the behavior of various oxides formed during the ablation.

### Acknowledgments

The authors thank the Center of Material Science at National University of Defense Technology for assistance in SEM characterization and XRD analysis.

### References

- [1] Y.G. Tong, S.X. Bai, K. Chen, C/C–ZrC composite prepared by chemical vapor infiltration combined with alloyed reactive melt infiltration, *Ceramics International* 38 (2012) 5723–5730.
- [2] J.R. Strife, J.E. Sheehan, Ceramic coatings for carbon–carbon composites, *American Ceramic Society Bulletin* 67 (1988) 369–374.
- [3] J.E. Sheehan, Oxidation protection for carbon fibre composites, *Carbon* 27 (1989) 709–715.
- [4] Y.C. Zhu, S. Ohtani, Y. Sato, N. Iwamoto, Influence of boron ion implantation on the oxidation behavior of CVD-SiC coated carbon–carbon composites, *Carbon* 38 (2000) 501–507.
- [5] J.F. Huang, X.R. Zeng, H.J. Li, X.B. Xiong, M. Huang, Mullite-Al<sub>2</sub>O<sub>3</sub>–SiC oxidation protective coating for carbon/carbon composites, *Carbon* 41 (2003) 2825–2829.
- [6] Y. Wang, Y.D. Xu, Y.G. Wang, L.F. Cheng, L.T. Zhang, Effects of TaC addition on the ablation resistance of C/SiC, *Materials Letters* 64 (2010) 2068–2071.
- [7] E. Wuchina, E. Opila, W. Fahrenholtz, I. Talmy, UHTCs: ultra-high temperature ceramic materials for extreme environment applications, *The Electrochemical Society Interface Winter* (2007) 30–36.
- [8] L.H. Zou, N. Wali, J.M. Yang, N.P. Bansal, Microstructural development of a Cf/ZrC composite manufactured by reactive melt infiltration, *Journal of the European Ceramic Society* 30 (2010) 1527–1535.
- [9] <[http://www.ultramet.com/ceramic\\_protective\\_coatings.html](http://www.ultramet.com/ceramic_protective_coatings.html)>.
- [10] E.O. Einset, Analysis of reactive melt infiltration in the processing of ceramics and ceramic composites, *Chemical Engineering Science* 53 (1998) 1027–1039.
- [11] W. Krenkel, Cost effective processing of composites by melt infiltration (LSI process), *Ceramic Engineering and Science Proceedings* 22 (2001) 443–454.
- [12] Y. Wang, X.J. Zhu, L.T. Zhang, L.F. Cheng, Reaction kinetics and ablation properties of C/C–ZrC composites fabricated by reactive melt infiltration, *Ceramics International* 37 (2011) 1277–1283.
- [13] S.R. Levine, E.J. Opila, M.C. Halbig, Evaluation of ultra-high temperature ceramics for aeropropulsion use, *Journal of the European Ceramic Society* 22 (2002) 2757–2768.
- [14] D.L. Ye, *Handbook of Thermodynamic Data for Applied Inorganic Material*, The Metallurgical Industry Press, Beijing, 2002.